Project 1: Modelling, Analysis and Control of a Robotic Manipulator

Siddharth Narayanan

November 2021

Contents

List of Figures

List of Tables

Abstract

This report presents the dynamics and control of a 3DOF robotic arm. The robotic arm has 3 degrees of freedom and the Denavit-Hartenberg(DH) convention has been used to represent the link relationships to set up the forward and inverse kinematics of the manipulator. Lagrange's approach has been followed to establish the governing equations of motion. The trajectory of the robot has been constructed for the pick and place application discussed. Regulation control is implemented to check if the robot can hold its position. PD control techniques are implemented to track the desired trajectory. Robustness of the PD controller is demonstrated and a real time parameter updation technique is demonstrated using an adaptive controller to account for uncertainty in mass of the payload.

1 Introduction

Robotic manipulators find applications, in places where the operation gets repeated for a multitude of iterations. A 3DOF(Degree of Freedom) manipulator has been considered for the application of transferring objects between two conveyors. Such applications can most commonly be found in the production industry where material needs to be transferred between conveyors for different operations to take place. Automation of transfer between the conveyors can help reduce human involvement, thereby eliminating any associated safety hazards that come along with it. Figure 1 presents a schematic design of the system with the robotic manipulator. The application can be described as follows with the following considerations,

1. An industrial production line making cold drinks is considered. All these cold drinks be packaged in similarly sized cans.
2. The cans are then packaged into larger carton boxes with the number of cans per carton box remaining constant such that the total weight of each carton has negligible variation.
3. These carton boxes are then placed into conveyor 2, which transfer the carton boxes to the next part of the production line.
4. The manipulator considered is used to transfer these cartons from conveyor 2 to a bin in conveyor 1 as shown in the figure.
5. The palletized carton boxes are transferred to the freezing units(warehouse) through conveyor 1.

The trajectory of the robot is defined for the application considered. With the robot being pick and place, there is need for the robot to hold it's position when it is picking up and placing the carton box. This is demonstrated by using a regulation control algorithm which is used to make the robot hold a specific position. The actual trajectory of the robot needs to match the desired trajectory. This is accomplished by using a PD-Controller. A computed torque and a modified computed torque control has been presented for this purpose. The mass of the payload(carton box) is not always the same. There is always some uncertainty in the mass of the payload considered. A real parameter adaptation law has been implemented to account for the uncertainty and helps the robot to trace the desired path.

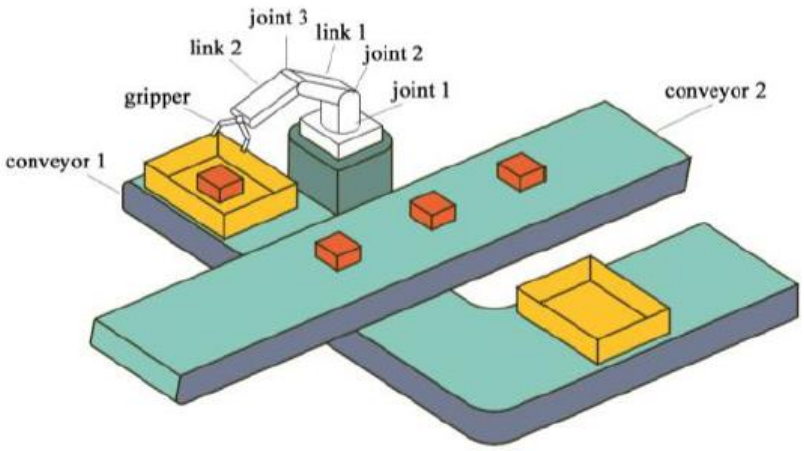

Figure 1: System Design

1.1 Other applications

Pick and place robots can be used for a wide variety of applications other than the one presented. A few examples are listed below.

1. **Assembly lines:** They can be used to pick components from an incoming line and place/fix or assemble it with another component.
2. **Warehousing:** Pick and place robots can be used to pick pallets or bins and store them in the desired storage locations. They can also be used to stack bins over one another.
3. **Quality Control:** They can be used to remove defective parts from the production line before it reaches the next stage of production/assembly.
4. **Loading into truck and containers:** They can be used to load finished components in pallets/bins into transportation containers and trucks.

2 Process methodology

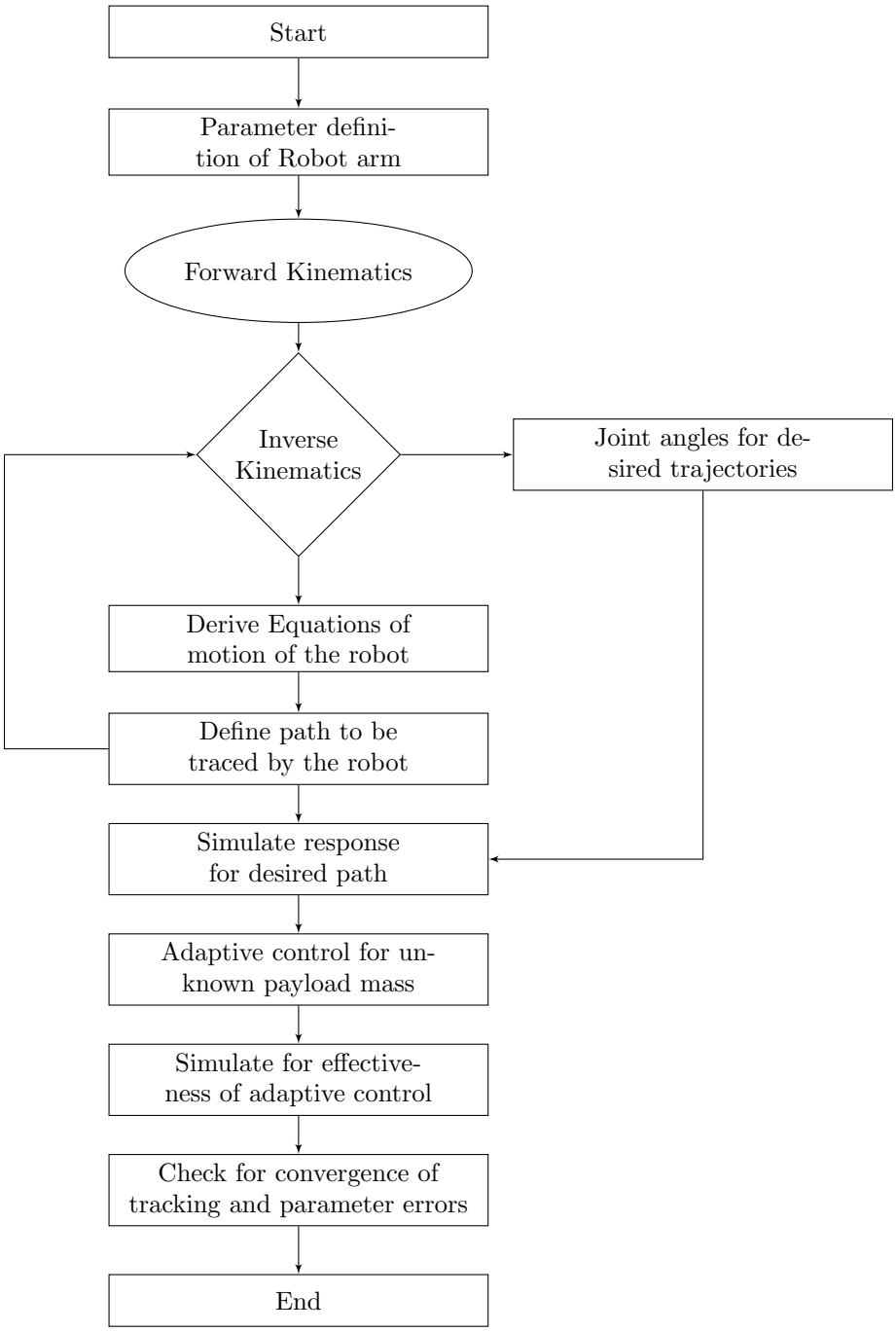

3 Parameter Definition of the robot arm

The robotic arm considered is presented in Figure below. All 3 joints are revolute, making the robotic arm have 3 rotational degrees of freedom. The mass of the payload to be lifted is consistently assumed to be 30±0.01 kgs. The weight variation between consecutive payloads is thus assumed to be little to negligible. The 3 links are assumed to be of length 1m, 1m and 1m respectively and that their weight is evenly distributed through their length. This constrains the centre of masses to be at the middle of the links at distances 0.5m, 0.5m, 0.5m respectively. The masses of the links are summed to be 110, 100 and 125kg respectively. This weight is inclusive of all the structures, the electrical and pneumatics that come along with it. There is a pneumatic gripper at the end of the 3^{rd} link which accomplishes the pick and place operations. It is assumed that the size and shape of the boxes are fixed, and the process is well controlled making the orientation of the carton similar so that the need of a spherical wrist is eliminated. Figure (2) shows a 3D representation of the robotic arm considered. Solidworks has been used to model the figure.

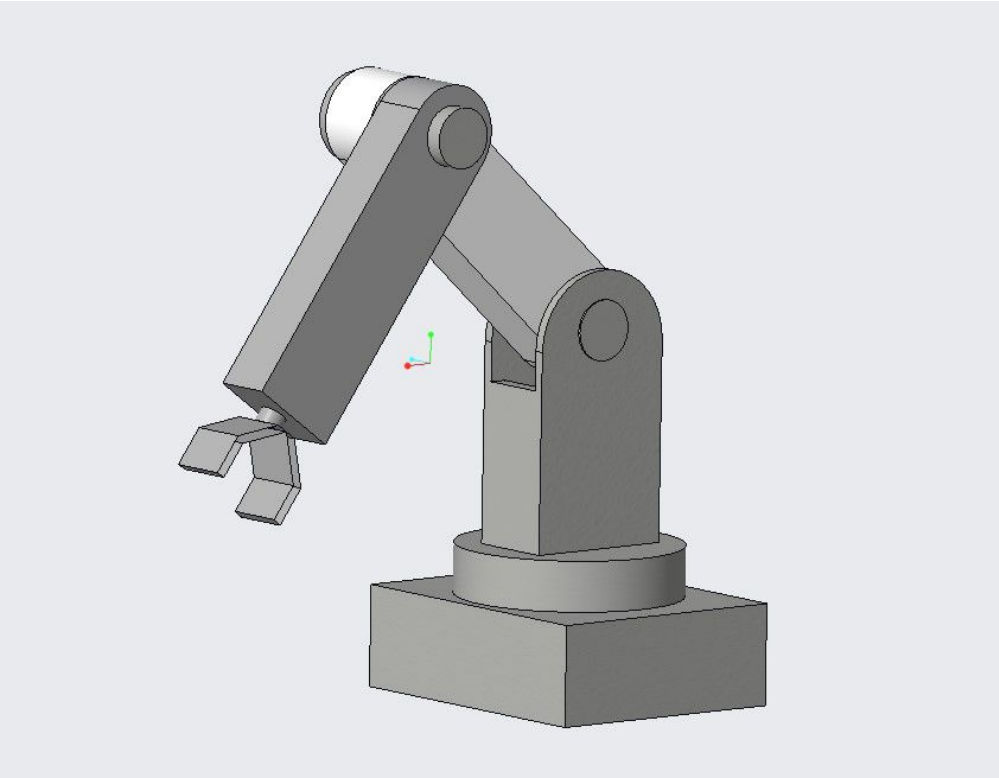

Figure 2: Robotic arm

4 Forward Kinematics

The position of the end-effector of the robot is computed using the kinematic equations of the robot with the specified joint values. This is the forward kinematics problem.
The robotic manipulator considered has 3 links. Frames are attached to each of the links of the robot. The Denavit-Hartenberg convention is used to attach the frames to each link of the robot. We have a ground frame $\mathcal{F}_0$ attached to the base of the manipulator. Links $\mathcal{F}_1$, $\mathcal{F}_2$, $\mathcal{F}_3$ are attached to links 1, 2 and the end effector of the manipulator. The DH Convention describes the relationships between the links using 4 variables θ, d, α and a where

$\theta \longrightarrow$ Angle of rotation to align x_{i-1} with x_i about z_{i-1}

$d_i \longrightarrow$ Translation along z_{i-1} to reach z_i

$a_i \longrightarrow$ Translation along x_i from x_{i-1}

$\alpha \longrightarrow$ Angle of rotation to align z_{i-1} with z_i about x_i

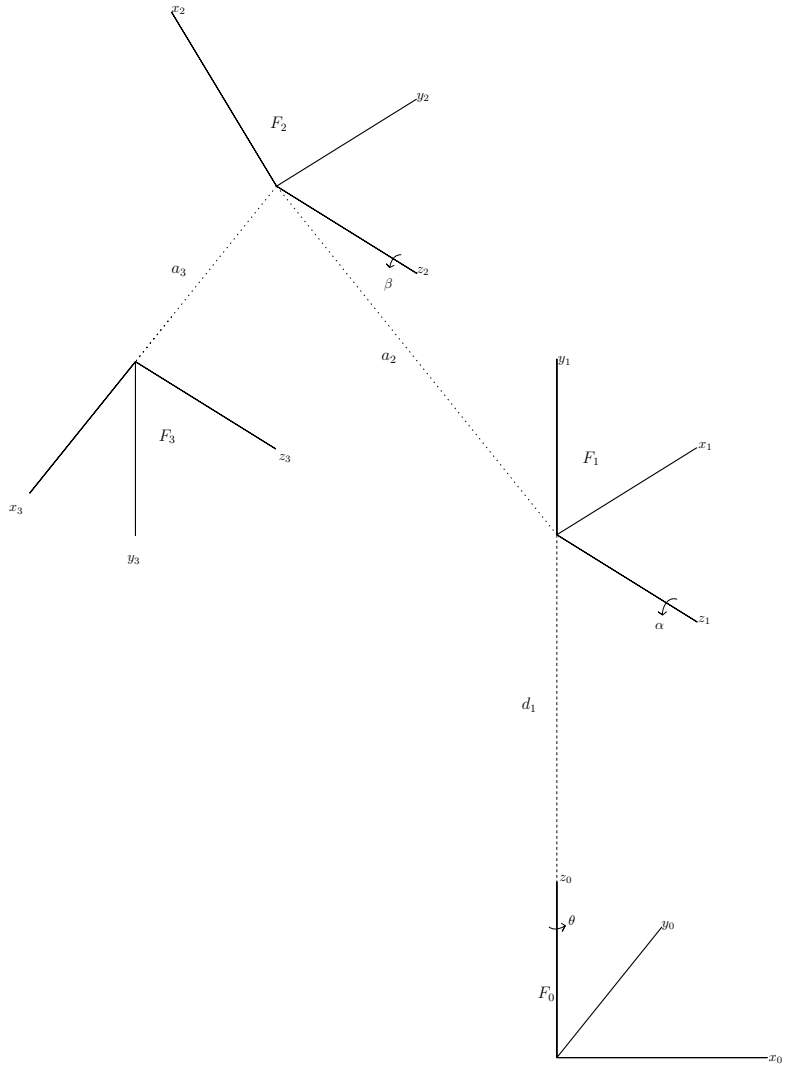

Figure 3: Axis representation of the robot

Link	θ	d_i	a_i	α
1	θ^*	d_1	0	$\pi/2$
2	α^*	0	a_2	0
3	β^*	0	a_3	0

Table 1: DH representation of the Robot

$$T_{i-1}^{i} = T_z(\theta)T_z(d)T_x(\alpha)T_x(a) \tag{1}$$

$$= \begin{bmatrix} c\theta & -s\theta & 0 & 0 \\ s\theta & c\theta & 0 & 0 \\ 0 & 0 & 1 & 0 \\ 0 & 0 & 0 & 1 \end{bmatrix} \begin{bmatrix} 1 & 0 & 0 & 0 \\ 0 & 1 & 0 & 0 \\ 0 & 0 & 1 & d \\ 0 & 0 & 0 & 1 \end{bmatrix} \begin{bmatrix} 1 & 0 & 0 & 0 \\ 0 & c\alpha & s\alpha & 0 \\ 0 & -s\alpha & c\alpha & 0 \\ 0 & 0 & 0 & 1 \end{bmatrix} \begin{bmatrix} 1 & 0 & 0 & a \\ 0 & 1 & 0 & 0 \\ 0 & 0 & 1 & 0 \\ 0 & 0 & 0 & 1 \end{bmatrix} \tag{2}$$

$$= \begin{bmatrix} c\theta & -s\theta c\alpha & s\theta s\alpha & ac\theta \\ s\theta & c\theta c\alpha & -c\theta s\alpha & as\theta \\ 0 & s\alpha & c\alpha & d \\ 0 & 0 & 0 & 1 \end{bmatrix} \tag{3}$$

This equation 1 represents the transformation of the i^{th} link with respect to the $(i-1)^{th}$ link.

The composite transformation of the end effector with the ground frame $\mathcal{F}_0$ is given by

$$\begin{aligned} T_0^3 &= T_0^1 T_1^2 T_2^3 \\ T_0^3 &= T_z(\theta^*)T_z(d_1)T_x(\pi/2)T_z(\alpha^*)T_x(a_2)T_z(\beta^*)T_x(a_3) \\ &= \begin{bmatrix} c\theta^*(c\alpha^*\beta^*) & -c\theta^*(s\alpha^*\beta^*) & s\theta^* & c\theta^*(a_2 + a_3 c\alpha^*) \\ s\theta^*(c\alpha^*\beta^*) & -s\theta^*(s\alpha^*\beta^*) & -c\theta^* & c\theta^*(a_2 + a_3 c\alpha^*) \\ s\alpha^*\beta^* & c\alpha^*\beta^* & 0 & a_3 s\alpha^* + d_1 \\ 0 & 0 & 0 & 1 \end{bmatrix} \end{aligned} \tag{4}$$

This equation 4 gives the relationship of the end effector with respect to the ground frame $\mathcal{F}_0$.

5 Inverse Kinematics

Inverse kinematics uses the final position of the end effector to get the joint angles of robot. This can be used to find the angles of the joints for the given position for the end effector. A robot can have different joint angles top achieve the same pose and orientation. The best solution can then be chosen to achieve the desired configuration depending on the robot.

$$\begin{aligned} T_0^3 &= T_0^1 T_1^2 T_2^3 \\ T_0^3 &= T_z(\theta^*) T_z(d_1) T_x(\pi/2) T_z(\alpha^*) T_x(a_2) T_z(\beta^*) T_x(a_3) \end{aligned} \tag{5}$$

The position of the end effector in $\mathcal{F}_0$ is given by ($\bar{x}$,$\bar{y}$,$\bar{z}$).

$$\begin{bmatrix} \bar{x} \\ \bar{y} \\ \bar{z} \\ 1 \end{bmatrix} = T_z(\theta^*) T_z(d_1) T_x(\pi/2) T_z(\alpha^*) T_x(a_2) T_z(\beta^*) T_x(a_3) \tag{6}$$

Moving the first rotation and translation to LHS,

$$\begin{aligned} T_z(-\theta^*) \begin{bmatrix} \bar{x} \\ \bar{y} \\ \bar{z} - d_1 \\ 1 \end{bmatrix} &= T_x(\pi/2) T_z(\alpha^*) T_x(a_2) T_z(\beta^*) T_x(a_3) \\ &= \begin{bmatrix} a_2 c\alpha + a_3 c\alpha\beta \\ 0 \\ a_2 s\alpha + a_3 s\alpha\beta \\ 1 \end{bmatrix} = \begin{bmatrix} B_x \\ B_y \\ B_z \\ 1 \end{bmatrix} \end{aligned} \tag{7}$$

Applying invariance of rotation,

$$\bar{x}^2 + \bar{y}^2 = a_2 c\alpha + a_3 c\alpha\beta = L \tag{8}$$

$$\bar{z} - d1 = a_2 s\alpha + a_3 s\alpha\beta \tag{9}$$

$$a_3 c\alpha\beta = L - a_2 c\alpha \tag{10}$$

$$a_3 s\alpha\beta = \bar{z} - d_1 \tag{11}$$

Squaring and adding 10 and 11,

$$a_3^2 = L^2 + a_2^2 - 2a_2[Lc\alpha + (\bar{z} - d_1)s\alpha] + (\bar{z} - d_1)^2 \tag{12}$$

$$2a_2[Lc\alpha + (\bar{z} - d_1)s\alpha] = L^2 + a_2^2 + (\bar{z} - d_1)^2 - a_3^2 \tag{13}$$

$$Lc\alpha + (\bar{z} - d_1)s\alpha = \frac{L^2 + a_2^2 + (\bar{z} - d_1)^2 - a_3^2}{2a_2} \tag{14}$$

This is of the general form

$$Ac\phi + Bs\phi = C \tag{15}$$

Here C is given by,

$$C = \sqrt{A^2 + B^2} \tag{16}$$

14 can be written as,

$$\frac{Lc\alpha}{\sqrt{L^2+(\bar{z}-d_1)^2}}+\frac{(\bar{z}-d_1)s\alpha}{\sqrt{L^2+(\bar{z}-d_1)^2}}=\frac{L^2+a_2^2+(\bar{z}-d_1)^2-a_3^2}{2a_2\sqrt{L^2+(\bar{z}-d_1)^2}} \tag{17}$$

This can be written as,

$$c(\alpha-\gamma)=\frac{L^2+a_2^2+(\bar{z}-d_1)^2-a_3^2}{2a_2\sqrt{L^2+(\bar{z}-d_1)^2}} \tag{18}$$

The terms on the RHS of 18 are known. 18 gives two values of (α-γ). From this, two values of α can be found out.

8 and 9 can be re-written as,

$$\begin{bmatrix} a_3c\alpha & -a_3s\alpha \\ a_3s\alpha & a_3c\alpha \end{bmatrix}\begin{bmatrix} c\beta \\ s\beta \end{bmatrix}=\begin{bmatrix} L-a_2c\alpha \\ \bar{z}-d_1-a_2s\alpha \end{bmatrix} \tag{19}$$

19 gives two values of β for every value of α. Four sets of solutions for α and β can be found.

Consider 7 and by applying invariance of rotation,

$$\begin{bmatrix} c\theta & s\theta \\ -s\theta & c\theta \end{bmatrix}\begin{bmatrix} \bar{x} \\ \bar{y} \end{bmatrix}=\begin{bmatrix} B_x \\ B_y \end{bmatrix} \tag{20}$$

This can be rearranged into,

$$\begin{bmatrix} \bar{x} & \bar{y} \\ \bar{y} & -\bar{x} \end{bmatrix}\begin{bmatrix} c\theta \\ s\theta \end{bmatrix}=\begin{bmatrix} B_x \\ B_y \end{bmatrix} \tag{21}$$

θ can be found out from 21 by,

$$\begin{bmatrix} c\theta \\ s\theta \end{bmatrix}=\frac{1}{\bar{x}^2+\bar{y}^2}\begin{bmatrix} \bar{x} & \bar{y} \\ \bar{y} & -\bar{x} \end{bmatrix}\begin{bmatrix} B_x \\ B_y \end{bmatrix} \tag{22}$$

22 gives one value of θ for every set of (α, β).

Four sets of solutions of (θ, α, β) are obtained.

6 Equations of motion

The equations of motions of the robotic arm helps us define the motion of the robot as a function of time. These equations are defined in terms of certain dynamic variables of the system. These dynamic variables are called the generalised coordinates of the system. The Lagrangian route will be adopted to find the equations of motion of the robotic manipulator.
Consider m_1, m_2, m_3 to be the masses of the 3 links of the manipulator. Let I_1, I_2, I_3 be their respective moments of inertia about the principal axis. d_1, a_2, a_3 are the lengths of the links and a, b, g are the points along the link at which the centre of mass is concentrated. Let τ_1, τ_2, τ_3 be the torques applied to each of the links with a motor. The kinetic and potential energy of each of the links are calculated. The Lagrangian, is given by the sum of individual kinetic energies and the potential energy 'V' subtracted of it.

$$L = TotalKineticenergy(T) - Potentialenergy(V) \tag{23}$$

The kinetic energy of the body is split into two components i.e, one due to the translation motion of the arms and the other due to the rotational motion of the arms. These are the Translational Kinetic Energy(TKE) and Rotational Kinetic Energy(RKE) components respectively.

$$T = \sum_{n=1}^{3} TKE + \sum_{n=1}^{3} RKE \tag{24}$$

The translational kinetic energy depends on the motion of the object through space and is given by,

$$TKE = \frac{1}{2} * m_i * v_c^t * v_c \tag{25}$$

m_i is the mass of the link and the v_c is the velocity about the centre of the mass of the link.
The rotational kinetic energy depends on the rotation of the body about an axis and is given by,

$$RKE = \frac{1}{2} * \omega_c^t * I_i * \omega_c \tag{26}$$

ω is the angular velocity, I_i is the moment of inertia about the principal axis of the link.
Coordinate relationships are established between the links and the body frame ($\mathcal{F}_i$) and between the body frame($\mathcal{F}_i$) and ground frame ($\mathcal{F}_0$). This can be used to calculate the velocity about the centre of mass of the links. The axes are notated as x_i, y_i, z_i for link i where i = 0 - 3. The base frame($\mathcal{F}_0$) is defined by the the axes x_0, y_0, z_0. The subsequent link frames $\mathcal{F}_i$ are defined by the direction cosines of the link with respect to the base frame $\mathcal{F}_0$ or the previous frame $\mathcal{F}_{i-1}$.

$$\begin{aligned} x_1 &= c\theta x_0 + s\theta y_0 \\ y_1 &= z_0 \\ z_1 &= s\theta x_0 - c\theta y_0 \end{aligned} \tag{27}$$

The equation 27 shows the relationships between the first link and the base frame.

Similarly,

$$\begin{aligned} x_2 &= c\alpha x_1 + s\alpha y_1 \\ y_2 &= -s\alpha x_1 + c\alpha y_1 \\ z_2 &= z_1 \end{aligned} \tag{28}$$

$$\begin{aligned} x_3 &= c\beta x_2 + s\beta y_2 \\ y_3 &= -s\beta x_2 + c\beta y_2 \\ z_3 &= z_2 \end{aligned} \tag{29}$$

The equations 28 and 29 show the relationships of second and the third link with the previous link. The velocities of the centre of masses of the links can be found using the co-ordinate relationships,

6.1 Velocities of the links

Angular velocities of the links: The angular velocities of the links is given by ω_i where i is the index of the link. $\dot{\theta}$, $\dot{\alpha}$, $\dot{\beta}$ is the change in the angle of the link with respect to time. The angular velocity is the dot product of the change in the angular displacements with the axis of rotation.

$$\omega_1 = \dot{\theta} z_0 \tag{30}$$

$$\omega_2 = \dot{\theta} z_0 + \dot{\alpha} z_1 = \dot{\theta} y_1 + \dot{\alpha} z_2 \tag{31}$$

$$= \dot{\theta}(s\alpha x_2 + c\alpha y_2) + \dot{\alpha} z_2 \tag{32}$$

$$\omega_3 = \dot{\theta} y_1 + \dot{\alpha} z_3 + \dot{\beta} z_3 \tag{33}$$

$$= \dot{\theta}(s\alpha\beta x_3 + c\alpha\beta y_3) + (\dot{\alpha} + \dot{\beta}) z_3 \tag{34}$$

Linear Velocity of centre of mass of link 1 :

$$\begin{aligned} r_a &= a * y_1 \\ v_a &= a * \frac{dy_1}{dt} \\ &= a(\omega_1 \,\mathrm{x}\, y_1) \\ &= a(\dot{\theta} z_0 \,\mathrm{x}\, y_1) \\ &= 0 \end{aligned} \tag{35}$$

Linear Velocity of centre of mass of link 2 :

$$\begin{aligned} r_b &= d_1 * y_1 + b * x_2 \\ v_b &= d_1 * \frac{dy_1}{dt} + b * \frac{dx_2}{dt} \\ &= d_1(\omega_1 \,\mathrm{x}\, y_1) + b(\omega_2 \,\mathrm{x}\, x_2) \\ &= d_1(\dot{\theta} z_0 \,\mathrm{x}\, y_1) + b((\dot{\theta} z_0 + \dot{\alpha} z_1)\mathrm{x}\, x_2) \\ &= x_0(\dot{\theta} bc\alpha s\theta - \alpha bc\dot{\theta} s\alpha) \\ &+ y_0(-\dot{\theta} bc\alpha c\theta - \dot{\alpha} bs\alpha s\theta) \\ &+ z_0(-\dot{\alpha} bc\alpha) \end{aligned} \tag{36}$$

Linear Velocity of centre of mass of link 3 :

$$\begin{aligned} r_c &= d_1 * y_1 + a_2 * x_2 + g * x_3 \\ v_c &= d_1 * \frac{dy_1}{dt} + a_2 * \frac{dx_2}{dt} + g * \frac{dx_3}{dt} \\ &= x_1(-\dot{\alpha} a_2 s\alpha - \dot{\alpha} g s\alpha\beta - \dot{\beta} g s\alpha\beta) \\ &+ y_1(\dot{\alpha} a_2 c\alpha + \dot{\alpha} g c\alpha\beta + \dot{\beta} g c\alpha\beta) \\ &+ z_1(\dot{\theta} a_2 c\alpha - \dot{\theta} g c\alpha\beta) \end{aligned} \tag{37}$$

35 , 36, 37 give the linear velocities of the links 1, 2 and 3.

6.2 Kinetic Energies of the links

Translational Kinetic Energy of the links : The translational kinetic energy of the links are notated as TKE_i where i is the index of the link.
For link 1,

$$TKE_1 = \frac{1}{2} * m_1 * v_a^t * v_a = 0 \tag{38}$$

For link 2,

$$TKE_2 = \frac{1}{2} * m_2 * v_b^t * v_b = \frac{m_2}{2}(\dot{\theta}^2 b^2 c^2\alpha + \dot{\alpha}^2 b^2) \tag{39}$$

For link 3,

$$\begin{aligned} TKE_3 &= \frac{1}{2} * m_3 * v_c^t * v_c \\ &= \frac{m_3}{2}(\dot{\theta}^2(a_2 c\alpha - g c\alpha\beta)^2 + \dot{\alpha}^2(a_2^2 + g^2 + 2a_2 g c\beta) + \dot{\beta}^2 g^2 + \dot{\alpha}\dot{\beta}(2a_2 g c\beta + 2g^2)) \end{aligned} \tag{40}$$

38, 39, 40 give the translational kinetic energies of the links 1, 2 and 3.

Rotational Kinetic Energy of the links : The translational kinetic energy of the links are notated as RKE_i where i is the index of the link.
The Rotational kinetic energy of the links is given by,

$$RKE = \frac{1}{2} * \omega_c^t * I_i * \omega_c \tag{41}$$

Here

$$\omega_c = \begin{bmatrix} \omega_x \\ \omega_y \\ \omega_z \end{bmatrix} \tag{42}$$

And,

$$I_i = \begin{bmatrix} I_{xx} & 0 & 0 \\ 0 & I_{yy} & 0 \\ 0 & 0 & I_{zz} \end{bmatrix} \tag{43}$$

For link 1,

$$\begin{aligned} RKE_1 &= \frac{1}{2} * \omega_1^t * I_1 * \omega_1 \\ &= \frac{I_{yy_1}}{2}\dot{\theta}^2 \end{aligned} \tag{44}$$

For link 2,

$$\begin{aligned} RKE_2 &= \frac{1}{2} * \omega_2^t * I_2 * \omega_2 \\ &= \frac{I_{xx_2}}{2}\dot{\theta}^2 s^2\alpha + \frac{I_{yy_2}}{2}\dot{\theta}^2 c^2\alpha + \frac{I_{zz_2}}{2}\dot{\alpha}^2 \end{aligned} \tag{45}$$

For link 3,

$$\begin{aligned} RKE_3 &= \frac{1}{2} * \omega_3^t * I_3 * \omega_3 \\ &= \frac{I_{xx_3}}{2}\dot{\theta}^2 s^2\alpha\beta + \frac{I_{yy_3}}{2}\dot{\theta}^2 c^2\alpha\beta + \frac{I_{zz_3}}{2}(\dot{\alpha}+\dot{\beta})^2 \end{aligned} \tag{46}$$

6.3 Potential energy of the system

The potential energy is the energy stored by the link by virtue of its position relative to the base frame. The potential energy is given by

$$Potential\, energy(V) = m_i * 9.81 * z_i \tag{47}$$

m_i is the mass of the link and z_i is the height of the link with respect to the base link $\mathcal{F}_\prime$.
For link 1,

$$V_1 = m_1 * 9.81 * d_1 \tag{48}$$

For link 2,

$$\begin{aligned} V_2 &= m_2 * 9.81 * z_2 \\ z_2 &= R_0^2 * [Coordinates\, in\, F_2] \\ &= \begin{bmatrix} c\theta\alpha & -c\alpha & s\theta \\ s\alpha & -s\theta s\alpha & -c\theta \\ s\alpha & c\alpha & 0 \end{bmatrix} \begin{bmatrix} a_2 \\ 0 \\ 0 \end{bmatrix} \\ &= \begin{bmatrix} 0 \\ 0 \\ a_2 s\alpha \end{bmatrix} \\ V_2 &= m_2 9.81 a_2 s\alpha + m_2 9.81 d_1 \end{aligned} \tag{49}$$

For link 3,

$$\begin{aligned}
V_3 &= m_3 9.81 z_3 \\
z_3 &= R_0^3 * [Coordinates\ in\ F_3] \\
&= \begin{bmatrix} c\theta(c\alpha\beta) & -c\theta^*(s\alpha\beta) & s\theta \\ s\theta(c\alpha\beta) & -s\theta(s\alpha\beta) & -c\theta \\ s\alpha\beta & c\alpha\beta & 0 \end{bmatrix} \begin{bmatrix} a_3 \\ 0 \\ 0 \end{bmatrix} \\
&= \begin{bmatrix} 0 \\ 0 \\ a_3 s\alpha\beta \end{bmatrix} \\
V_3 &= m_3 9.81 a_2 s\alpha + m_3 9.81 d_1 + m_3 9.81 a_3 s\alpha\beta
\end{aligned} \tag{50}$$

6.4 Lagrangian

The Lagrangian is then formulated with the calculated energies. The Lagrangian is the difference between the total kinetic energy and the total potential energy.

$$\begin{aligned}
L &= T - V \\
&= \frac{\dot{\theta}^2}{2}[m_2 b^2 c^2\alpha + m_3(a_2 c\alpha - g c\alpha\beta)^2 + I_{yy_1} + I_{xx_2} s^2\alpha + I_{yy_2} c^2\alpha + I_{xx_3} s^2\alpha\beta + I_{yy_3} c^2\alpha\beta] \\
&+ \frac{\dot{\alpha}^2}{2}[m_2 b^2 + m_3 a_2^2 + m_3 g^2 + 2 m_3 a_2 g c\beta + I_{zz_2} + I_{zz_3}] + \frac{\dot{\beta}^2}{2}[m_3 g^2 + I_{zz_3}] \\
&+ \dot{\alpha}\dot{\beta}[m_3 a_2 g c\beta + m_3 g^2] - 9.81 m_1 d_1 - 9.81 m_2 d_1 - 9.81 m_2 a_2 s\alpha - 9.81 m_3 d_1 - 9.81 m_3 a_2 s\alpha - 9.81 m_3 a_3 s\alpha\beta
\end{aligned} \tag{51}$$

51 is the simplified and expanded Lagrangian form obtained from the energies. This Lagrangian can be subsequently used to find the equations of motion of the robotic manipulator. The system here has 3 variables and hence there are three equations of motion. The equations of motion is given by

$$\begin{aligned}
\frac{d}{dt}\left(\frac{\partial L}{\partial \dot{\theta}}\right) - \frac{\partial L}{\partial \theta} &= \tau_1 \\
\frac{d}{dt}\left(\frac{\partial L}{\partial \dot{\alpha}}\right) - \frac{\partial L}{\partial \alpha} &= \tau_2 \\
\frac{d}{dt}\left(\frac{\partial L}{\partial \dot{\beta}}\right) - \frac{\partial L}{\partial \beta} &= \tau_3
\end{aligned} \tag{52}$$

52 defines the equations of motion for the robotic manipulator. The equations of motion are evaluated to be as follows :

EOM 1

$$\begin{aligned}
&= \ddot{\theta}[m_2 b^2 c^2\alpha + m_3(a_2 c\alpha - g c\alpha\beta)^2 + I_{yy_1} + I_{xx_2} s^2\alpha + I_{yy_2} c^2\alpha + I_{xx_3} s^2\alpha\beta + I_{yy_3} c^2\alpha\beta] \\
&+ \dot{\theta}[s(2\alpha)\dot{\alpha}(I_{xx_2} - I_{yy_2} - m_2 b^2 - m_3 a_2^2] + s(2\alpha\beta)(\dot{\alpha} + \dot{\beta})(I_{xx_3} - I_{yy_3} - m_3 g^2) \\
&+ 2 a_2 g m_3 s\alpha\beta c\alpha(\dot{\alpha} + \dot{\beta}) + 2\dot{\alpha} a_2 g m_3 s\alpha\beta] = \tau_1
\end{aligned} \tag{53}$$

EOM 2

$$\begin{aligned}&= \ddot{\alpha}[m_2b^2 + m_3a_2^2 + m_3g^2 + 2m_3a_2gc\beta + I_{zz_2} + I_{zz_3}] + \frac{\dot{\beta}^2}{2}[m_3g^2 + I_{zz_3}] + \ddot{\beta}[m_3a_2gc\beta + m_3g^2] \\ &+ \dot{\alpha}\dot{\beta}(-2m_3a_2gs\beta) + \dot{\beta}^2[-m_3a_2gs\beta] - \ddot{\theta}^2[s\alpha c\alpha(I_{xx_2} - I_{yy_2} - m_2b^2) + s\alpha\beta c\alpha\beta(I_{xx_3} - Iyy_3 - m_3g^2) \\ &+ m_3a_2g(s\alpha\beta + c\alpha s\alpha\beta)] + 9.81m_2a_2c\alpha + 9.81m_3a_2c\alpha + 9.81m_3a_3c\alpha\beta = \tau_2\end{aligned} \tag{54}$$

EOM 3

$$\begin{aligned}&= \ddot{\beta}[m_3g^2 + I_{zz_3}] + \ddot{\alpha}[a_2gc\beta + g^2] - \ddot{\theta}^2[s\alpha\beta c\alpha\beta(I_{xx_3} - I_{yy_3} - m_3g^2) + a_2gm_3c\alpha s\alpha\beta] + \dot{\alpha}^2[m_3a_2gs\beta] \\ &+ 9.81m_3a_3c\alpha\beta = \tau_3\end{aligned} \tag{55}$$

53, 54 , 55 are the equations of the robotic manipulator. τ_1, τ_2 ,τ_3 are the control torques of the motors controlling the joint angles θ, α, β. The trajectory of the robotic manipulator can be controlled by these torques.

6.5 General form of Equations of Motion

The equations of motion are put into the form,

$$M(q)\ddot{q} + C(q,\dot{q})\dot{q} + G(q) = \tau \tag{56}$$

In 68 , M is the mass matrix , C is the Coriolis matrix and G is the potential energy matrix. Q is the matrix of the control torques. Energy is conservative if M and C are picked in a way such that $\dot{M}$-2C is skew symmetric. From 53, 54, 55, M, C and G are determined to be as follows:

$$M = \begin{bmatrix} m_2b^2c^2\alpha + m_3(a_2c\alpha - gc\alpha\beta)^2 + I_{yy_1} + I_{xx_2}s^2\alpha + \\ I_{yy_2}c^2\alpha + I_{xx_3}s^2\alpha\beta + I_{yy_3}c^2\alpha\beta & 0 & 0 \\ 0 & m_2b^2 + m_3a_2^2 + m_3g^2 + \\ & 2m_3a_2gc\beta + I_{zz_2} + I_{zz_3} & m_3a_2gc\beta + m_3g^2 \\ 0 & m_3a_2gc\beta + m_3g^2 & m_3g^2 + I_{zz_3} \end{bmatrix} \tag{57}$$

$$C = \begin{bmatrix} C_{11} & C_{12} & C_{13} \\ C_{21} & C_{22} & C_{23} \\ C_{31} & C_{32} & C_{33} \end{bmatrix} \tag{58}$$

where,

$$
\begin{aligned}
C_{11} &= s\alpha c\alpha\dot{\alpha}(I_{xx_2} - I_{yy_2} - m_2b^2 - m_3a_2^2) + c\alpha\beta s\alpha\beta(\dot{\alpha}+\dot{\beta})(I_{xx_3} - I_{yy_3} - m_3g^2) \\
&\quad + a_2gm_3s\alpha\beta c\alpha(\dot{\alpha}+\dot{\beta}) + a_2gm_3s\alpha c\alpha\beta\dot{\alpha} \\
C_{12} &= s\alpha c\alpha\dot{\theta}(I_{xx_2} - I_{yy_2} - m_2b^2 - m_3a_2^2) + s\alpha\beta c\alpha\beta\dot{\theta}(I_{xx_3} - I_{yy_3} - m_3g^2) \\
&\quad + (m_3a_2gs\alpha c\alpha\beta + m_3a_2gc\alpha s\alpha\beta)\dot{\theta} \\
C_{13} &= s\alpha\beta c\alpha\beta\dot{\theta}(I_{xx_3} - I_{yy_3} - m_3g^2) + \dot{\theta}(a_2gm_3s\alpha\beta c\alpha) \\
C_{21} &= -[s\alpha c\alpha\dot{\theta}(I_{xx_2} - I_{yy_2} - m_2b^2 - m_3a_2^2) + s\alpha\beta c\alpha\beta\dot{\theta}(I_{xx_3} - I_{yy_3} - m_3g^2) \\
&\quad + (m_3a_2gs\alpha c\alpha\beta + m_3a_2gc\alpha s\alpha\beta)\dot{\theta}] \\
C_{22} &= -m_3a_2gs\beta\dot{\beta} \\
C_{23} &= -m_3a_2gs\beta\dot{\alpha} - a_2gs\beta m_3\dot{\beta} \\
C_{31} &= -[s\alpha\beta c\alpha\beta\dot{\theta}(I_{xx_3} - I_{yy_3} - m_3g^2) + \dot{\theta}(a_2gm_3s\alpha\beta c\alpha)] \\
C_{32} &= m_3a_2gs\beta\dot{\alpha} \\
C_{33} &= 0
\end{aligned}
\tag{59}
$$

$$
G = \begin{bmatrix} 0 \\ 9.81m_2a_2c\alpha + 9.81m_3a_2c\alpha + 9.81m_3a_3c\alpha\beta \\ 9.81m_3a_3c\alpha\beta \end{bmatrix} \tag{60}
$$

$\dot{M}$-$2C$ is skew symmetric.

7 Path planning of the robot

The equations of motion of the robotic manipulator has been set up and now the robot trajectories are to be defined for the application presented. For the purpose of simplifying the problem, the following considerations are made,

- The pickup location is desired to be the initial location of the robot.There is a small error in position and velocity at the start of the first trial run.
- The robot has to be stationary when it is picking up and placing the component(carton box) respectively. The velocity of the links at these points is therefore, zero.
- The coordinate of the point of pick up and the coordinate of the point of placing is assumed to be on the same plane.
- An obstacle whose dimensions are known, if considered can be circumvented by making a manipulation in angle α of the manipulator. This enables the end effector to avoid the obstacle by height.
- The carton box is assumed to be of size 1m x 0.5m x 1m and is assumed to weigh 30 kgs.
- The points of picking up and placing are defined with respect to the base frame $\mathcal{F}_0$. The inverse kinematic solutions of these points should give the joint angles at these respective points.
- A general polynomial is the used as the characteristic equation of these joint angles and with the initial and final constraints on the joint angles and velocities along with intermediary conditions,the desired trajectory of the robot is defined.
- The gripper at the end of the third link is assumed to have its centre at the origin of $\mathcal{F}_3$.

7.1 Work space of the robot

Figure 4 shows the initial and final pick and drop points of the robot. The trajectory to be traced by the robot is shown by the red dotted line and the blue box represents the carton to be picked by the robot. All positions are defined with respect to the object base frame $\mathcal{F}_0$. Let O be the the origin of $\mathcal{F}_0$.

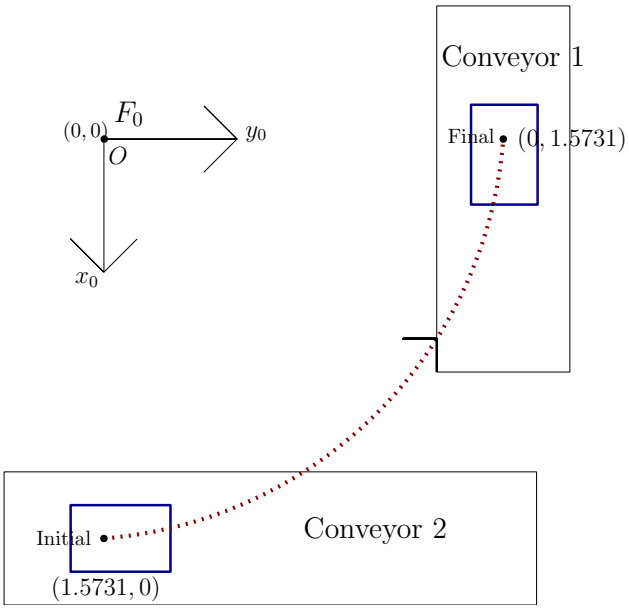

Figure 4: Trajectory of robot - Top view

With the assumption that the height of the carton box is 1m, it is assumed that the gripper needs a clearance of 0.2m to grip the box effectively. Therefore the initial and final locations of the end effector frame $\mathcal{F}_3$ are at heights of 1.2m in the z_0 direction. An obstacle of size 0.2 x 0.2 x 0.2 m at (1.0607, 1.0607, 0) in the frame $\mathcal{F}_0$ can be considered.
The location of the end effector coordinates are then fed into the inverse kinematics problem in MATLAB and four solutions are obtained. Only one of these solutions can be effectively used as the same end effector position can be obtained in multiple ways and only one solution facilitates the picking up of the component from the top.
For example, considering the initial point to be reached in the 3D space, we obtain a set of two solutions. One of the solutions positions the end effector in a way such that end effector is pointing upward though the same coordinate is reached. This solution is discarded as it can not accomplish the required operation. From figure 5, the second solution with position of end effector E_1 is discarded.

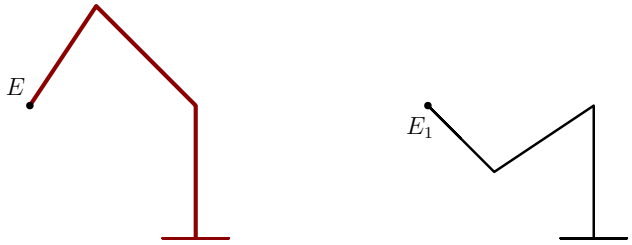

Figure 5: Inverse kinematic solutions

7.2 Desired trajectory

1. The defined trajectory is for a time period of 5 seconds. It is assumed that the end effector at t=0 is in position to pick up the payload. The robot lifts up the payload in order for the payload to have sufficient clearance from the ground.

2. The robot traverses from the initial point to the final point in 2 seconds, i.e it reaches the drop of location at t=2.

3. The robot is then assumed to stay at the position for one second.

4. The robot returns back to the initial point in 2 seconds again, i.e from t=3 to t=5.

5. The trajectory is chosen in a way such that the robot is ready to pick up the next carton when t=5. So the initial and final location of the robot will be the same.

6. In actual operation, the robot will have a brief pause between coming back to its initial position and picking up the next object. However for the purpose of trajectory generation, it is assumed that the line is operating at capacity with the robot needing to operate continuously to prevent bottlenecks.

7. The joint angles of the robot are summarised below.

Variable	Angle
θ	0
α	$3\pi/4$
β	$5\pi/12$

Table 2: Initial joint angles of the robot

Variable	Angle
θ	0
α	$3\pi/4$
β	$5\pi/12$

Table 3: Final joint angles of the robot

Time(s)	θ	α	β
1	$\pi/4$	$2\pi/3$	$\pi/3$
2	$\pi/2$	$3\pi/4$	$5\pi/12$
3	$\pi/2$	$3\pi/4$	$5\pi/12$
4	$\pi/4$	$2\pi/3$	$\pi/3$

Table 4: Joint angles of the robot

The velocities of the links are 0 at the initial and final positions. The velocities are negative at t=4 Velocities in the intermediary times are assumed as follows

Time(s)	$\dot{\theta}$	$\dot{\alpha}$	$\dot{\beta}$
1	0	0	0
2	1	0.1	0.1
3	0	0	0
4	-1	-0.1	-0.1

Table 5: Joint velocities of the robot

A 9^{th} degree polynomial is then considered to accommodate the 8 constraints used i.e, 4 joint positions and 4 joint velocities for each joint angle.

$$\theta(t) = p_0 + p_1 t + p_2 t^2 + p_3 t^3 + p_4 t^4 + p_5 t^5 + p_6 t^6 + p_7 t^7 + p_8 t^8 + p_9 t^9 \tag{61}$$

$$\alpha(t) = q_0 + q_1 t + q_2 t^2 + q_3 t^3 + q_4 t^4 + q_5 t^5 + q_6 t^6 + q_7 t^7 + q_8 t^8 + q_9 t^9 \tag{62}$$

$$\beta(t) = r_0 + r_1 t + r_2 t^2 + r_3 t^3 + r_4 t^4 + r_5 t^5 + r_6 t^6 + r_7 t^7 + r_8 t^8 + r_9 t^9 \tag{63}$$

Time derivatives of 61, 62 , 63 give the velocities of the joint angles. These equations are solved in MATLAB to get equations for the desired trajectories. They are denoted as θ_{des}(t), α_{des}(t), β_{des}(t) and their time derivatives respectively.(Time derivatives denote the desired joint velocities).The coordinates of the end effector at the different times are given by forward kinematics,

Time(s)	x	y	z
1	1.0607	1.0607	1.866
2	0	1.5731	1.2071
3	0	1.5731	1.2071
4	1.0607	1.0607	1.866

Table 6: End effector positions

An obstacle of size 0.2 x 0.2 x 0.2 m at (1.0607, 1.0607, 0) in the frame $\mathcal{F}_0$ can be avoided using the given trajectory. This can be inferred from Table 6.

8 Control Techniques

The equations of motion govern the motion of the end effector with respect to the varying joint angles. The desired path to be followed by the robot is given the polynomial equation defined in the previous section. Since the application considered needs the same path to be traced repeatedly, it is possible to iterate the same equations for the required number of cycles. For achieving this necessary trajectories, the links are fitted with motor which provide a torque. This torque, in turn enables to control the joint angles and the position of the robot.

8.1 Regulation Problem

The robot when picking up or placing the payload should be able to hold the configuration. This is at most necessary for picking and placing the payload at the desired points. The regulation error is the position difference between the actual position and the desired position which the robot should hold. The regulation error is mathematically defined as,

$$\tilde{q} = q - q^* \tag{64}$$

Here q^* is assumed to be the configuration at which the potential energy of the manipulator is minimum. The general equations of motion of the manipulator when put in standard form is given by,

$$M(q)\ddot{\tilde{q}} + C(q,\dot{q})\dot{q} + G(q) = \tau \tag{65}$$

The control action is assumed to be achieved by a Proportional-Derivative(PD) type controller and the control input is given by,

$$\tau_{in} = -K_d(\dot{\tilde{q}}) - K_p\tilde{q} \tag{66}$$

The closed loop equation will be of standard form,

$$M(q)\ddot{\tilde{q}} + C(q,\dot{q})\dot{q} + G(q) = -K_d(\dot{\tilde{q}}) - K_p\tilde{q} \tag{67}$$

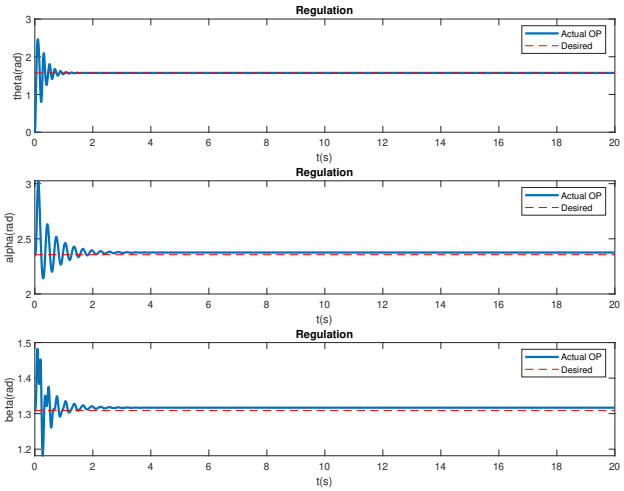

Figure 6: Regulation Plot

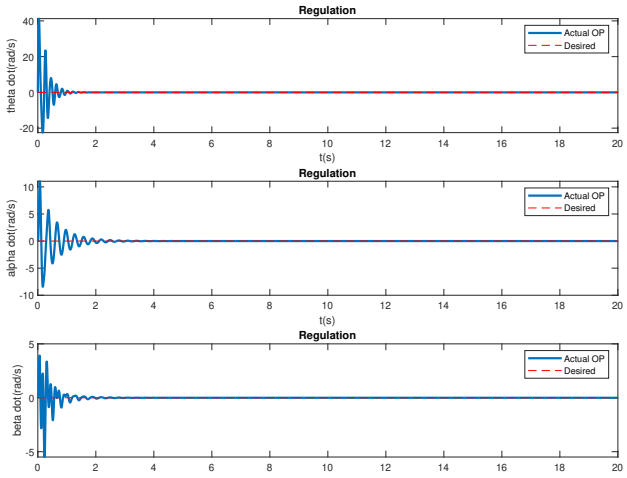

Figure 7: Regulation Plot

Observations: From Fig(6) and Fig(7), the position and velocity converge to the desired value in about 5 seconds. This simulation proves that the robot will be able to hold its position and velocity when lifting up the payload. Gains used on the controller to achieve this are K_p=40 and $K_d = 30$.

8.2 Tracking Problem

For the considered robotic arm, let τ_1, τ_2, τ_3 be the respective torques supplied by the motors to the links 1, 2 and 3 respectively. Any magnitude of torque provided will not accomplish the required trajectory that is to be traced by the robot. Therefore, the magnitude of torque supplied to the manipulator is to be controlled to make the robot track the necessary trajectory. This would be the tracking problem, which involves making the robot track the necessary desired trajectory.
Let us consider the equations of motion put in standard form,

$$M(q)\dot{\dot{q}} + C(q,\dot{q})\dot{q} + G(q) = \tau \tag{68}$$

Tracking error is the error between the actual value of joint angle or velocity with the desired values,

$$\tilde{q} = q(t) - q_{des}(t) \tag{69}$$

$$\dot{\tilde{q}} = \dot{q}(t) - \dot{q_{des}}(t) \tag{70}$$

In 69, 70, q and $\dot{q}$ represent the joint angles and velocities. The tracking problem tries to find the value of τ for which 69 and 70 is zero. There are a couple different control techniques through which these torques can be calculated making the tracking error go to zero.

8.2.1 Computed Torque Method

The computed torque control can be implemented as we have the dynamic model of the entire system. The computed torque model ensures that there is asymptotic stability. With asymptotic stability, the errors approach zero as the time tends to infinity.
The tracking error is given by 69 and 70 respectively. The control torque is given by the following equation,

$$\tau_{in} = M(q)\dot{\dot{q_{des}}} + C(q,\dot{q})\dot{q_{des}} + G(q) - K_p(\tilde{q}) - K_d(\dot{\tilde{q}}) \tag{71}$$

The closed loop equation put in standard form will be,

$$M(q)\dot{\dot{q}} + C(q,\dot{q})\dot{q} + G(q) = M(q)\dot{\dot{q}}_{des} + C(q,\dot{q})\dot{q}_{des} + G(q) - K_p(\tilde{q}) - K_d(\dot{\tilde{q}}) \tag{72}$$

Here K_p and K_d are the control gains associated with the computed torque controller. K_p is the proportional gain and K_d is the derivative gain. For the application considered,

$$\tilde{q} = \begin{bmatrix} \theta - \theta_{des} \\ \alpha - \alpha_{des} \\ \beta - \beta_{des} \end{bmatrix} \tag{73}$$

The time derivative of 73 will give $\dot{\tilde{q}}$. The computed torque control is implemented for the problem and the plots are obtained as follows,

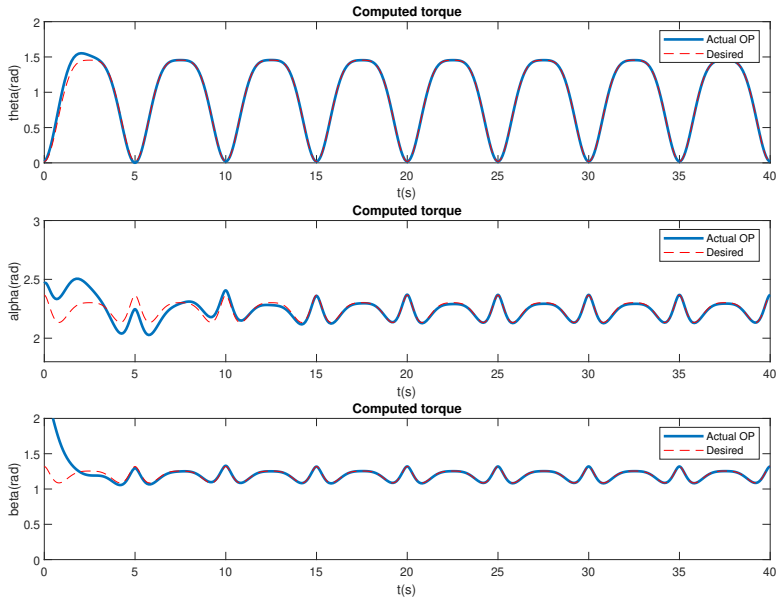

Figure 8: Position Plot- Computed Torque

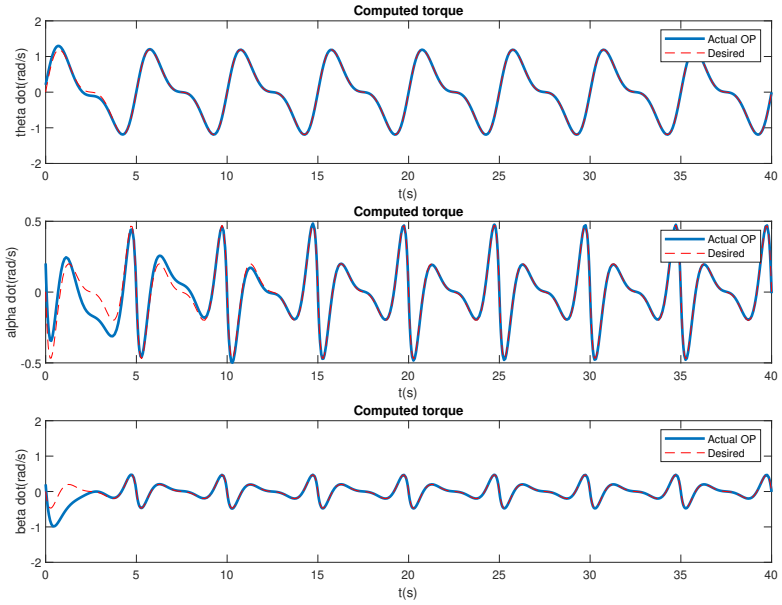

Figure 9: Velocity Plot- Computed Torque

Observations : The simulations from Fig(8) and Fig(9) show the simulations for the computed torque method. Initial position errors are assumed to be 0, 0.1, 1 rad for every joint angle and initial position error has been assumed to be 0.2 rad/s for every joint. The computed torque bring about the convergence of positions in about 15 seconds for all three joint angles. Convergence in velocity is achieved in 5 seconds. The robot arm traces the desired path with the desired velocity after 15 seconds. The gains for this controller is K_p=50 and K_d = 40.

8.2.2 Modified Computed Torque

The modified computed torque method is very similar to the computed torque method, but employs a composite error. The modified computed torque method also ensures asymptotic stability i.e, errors tend to zero as the time approaches infinity. The composite error is defined as

$$S = \dot{\tilde{q}} + \lambda \tilde{q} \tag{74}$$

For the purpose of simplification, we also define a reference velocity, $\dot{q_r}$ as,

$$\begin{aligned} \dot{q_r} &= \dot{q_{des}} - \lambda \tilde{q} \\ \tilde{q} &= q(t) - q_{des}(t) \end{aligned} \tag{75}$$

The control torque in this case is give by,

$$\tau_{in} = M(q)\dot{\dot{q_r}} + C(q, \dot{q})\dot{q_r} + G(q) - K_d S \tag{76}$$

The closed loop equation will be of form,

$$M(q)\dot{\dot{q}} + C(q, \dot{q})\dot{q} + G(q) = M(q)\dot{\dot{q_r}} + C(q, \dot{q})\dot{q_r} + G(q) - K_d S \tag{77}$$

The modified computed torque control is implemented for the application considered and the following plots are obtained,

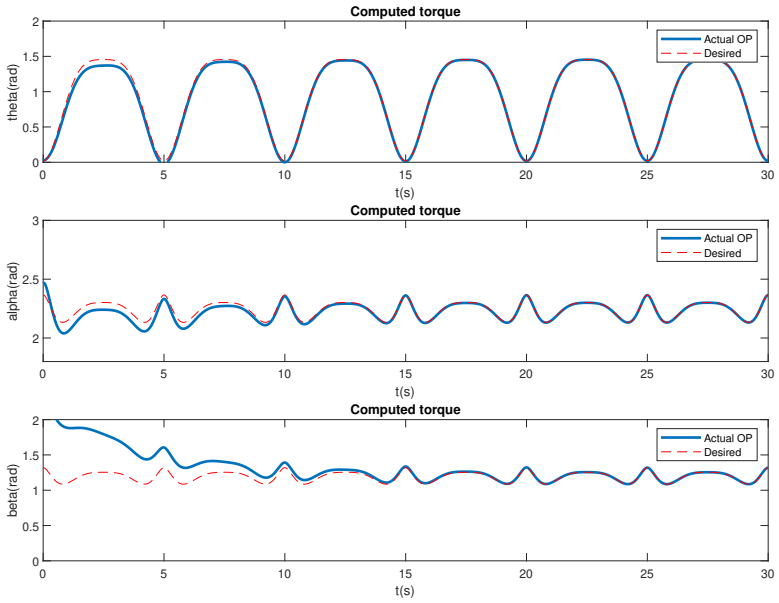

Figure 10: Position Plot- Modified Computed Torque

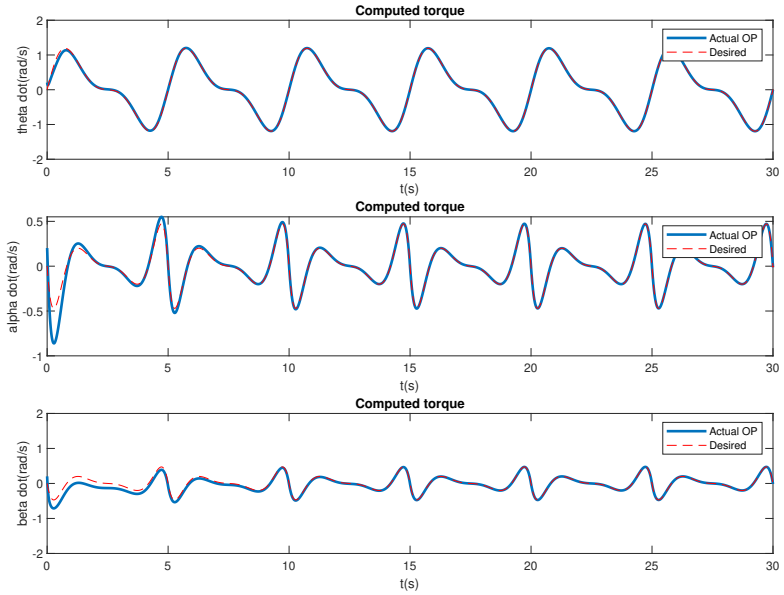

Figure 11: Velocity Plot- Modified Computed Torque

Observations : The simulations from Fig(10) and Fig(11) show the simulations for modified computed torque. Initial position errors are assumed to be 0, 0.1, 1 rad for every joint angle and initial position error has been assumed to be 0.2 rad/s for every joint. The modified computed torque bring about the convergence of positions in about 10 seconds for all three joint angles. Convergence in velocity is achieved in 5 seconds. The robot arm traces the desired path with the desired velocity after 10 seconds. The gains for this controller is λ=30 and $K_d = 20$.

8.2.3 Robustness

The discussion up until now and assumed that the parameters of the robot are known. Correspondingly, their trajectory has been modelled and their response has been plotted and studied. But in reality, we might not always know the parameters of the robot. There is some degree of uncertainty in the parameters of the robot. A controller is robust, if it is capable of accommodating the uncertainty and is still able to achieve convergence with the desired output. This can be simulated by modifying the mass m_3, and moment of inertia's of the third link and checking if the controller is able to stabilise the trajectory. We will consider the modified torque controller in this case.
The control torque in this case is give by,

$$\tau_{in} = M_1(q)\dot{\dot{q}}_r + C_1(q,\dot{q})\dot{q}_r + G_1(q) - K_d S \tag{78}$$

The closed loop equation will be of form,

$$M(q)\dot{\dot{q}} + C(q,\dot{q})\dot{q} + G(q) = M_1(q)\dot{\dot{q}}_r + C_1(q,\dot{q})\dot{q}_r + G_1(q) - K_d S \tag{79}$$

Here M_1, C_1, G_1 are modified matrices in which the mass m_3=180kgs, I_{xx_3} = 40kgm^2, I_{yy_3} = 60kgm^2, I_{zz_3} = 70kgm^2. The corresponding plots are obtained.

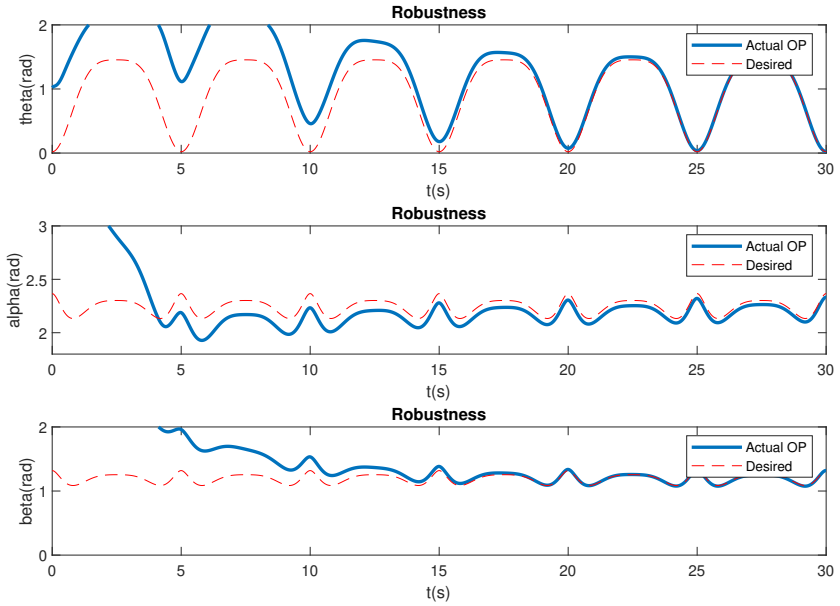

Figure 12: Position Plot- Robustness

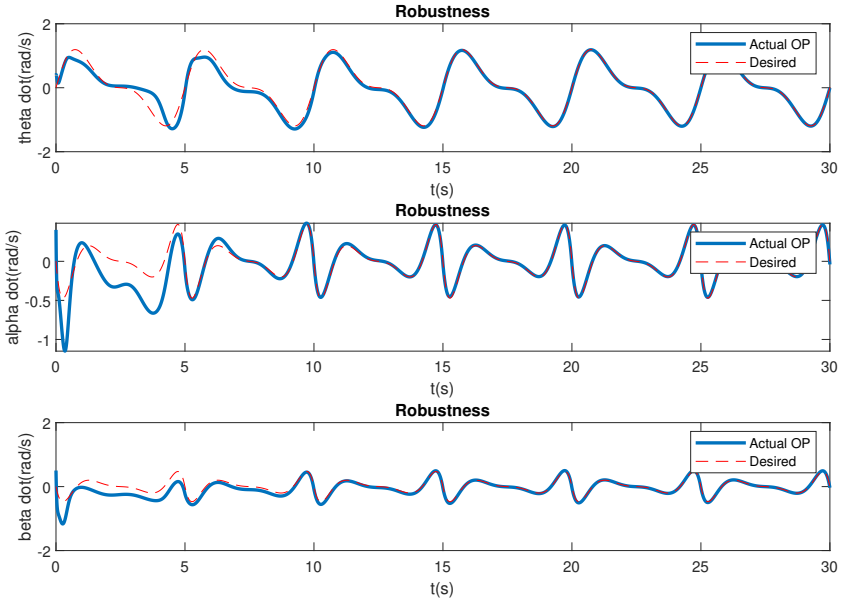

Figure 13: Velocity Plot- Robustness

Observations : The simulations from Fig(12) and Fig(13) show the simulations for the computed torque method. Initial position errors are assumed to be 1, 1.1, 2 rad for every joint angle and initial position error has been assumed to be 0.4, 0.4, 0.5 rad/s for every joint. The controller is able to achieve convergence with the desired trajectory and joint velocity in about 15 seconds. The controller is therefore able to account for the uncertainty in the parameters of the link. Gains in this case are obtained to be $\lambda = 30$ and K_d =20.

8.3 Adaptive Control

The whole discussion up until now has taken into account that the mass of payload is known. But the mass of the payload might not be known always or the mass of the payload can be different from the assumed mass. The uncertainty in the mass of the payload can be accounted by an adaptive controller. Here the the payload is considered to be a part of the 3^{rd} link and the whole mass of the 3^{rd} link is assumed to be a variable. The equation of motion is set up as follows,

$$\tau_{in} = Y_0 + Y_1\hat{m_3} + Y_2\hat{I_{xx_3}} + Y_3\hat{I_{yy_3}} + Y_4\hat{I_{zz_3}} - K_dS \tag{80}$$

where $\hat{m_3}$, $\hat{I_{xx_3}}$, $\hat{I_{yy_3}}$, $\hat{I_{zz_3}}$ are the unknown parameters. Best estimates of them are used. Y_0, Y_1, Y_2, Y_3, Y_4 are called the regressor vectors.

$$\hat{m_3} = -(S^TY_1)/\gamma_1 \tag{81}$$
$$\hat{I_{xx_3}} = -(S^TY_2)/\gamma_2 \tag{82}$$
$$\hat{I_{yy_3}} = -(S^TY_3)/\gamma_3 \tag{83}$$
$$\hat{I_{zz_3}} = -(S^TY_4)/\gamma_4 \tag{84}$$

Here γ_1, γ_2, γ_3, γ_4 are controller gains.

$$Y_0 = M_1(q)\dot{q_r} + C_1(q,\dot{q})\dot{q_r} + G_1(q) \tag{85}$$

Here,

$$M_1 = \begin{bmatrix} m_{11} & m_{12} & m_{13} \\ m_{21} & m_{22} & m_{23} \\ m_{31} & m_{32} & m_{33} \end{bmatrix} \tag{86}$$

$$\begin{aligned} m_{11} &= m_2 b^2 c^2\alpha + I_{yy_1} + I_{xx_2} s^2\alpha + I_{yy_2} c^2\alpha \\ m_{12} &= 0 \\ m_{13} &= 0 \\ m_{21} &= 0 \\ m_{22} &= m_2 b^2 + I_{zz_2} \\ m_{23} &= 0 \\ m_{31} &= m_{32} = m33 = 0 \end{aligned} \tag{87}$$

$$C_1 = \begin{bmatrix} c_{11} & c_{12} & c_{13} \\ c_{21} & c_{22} & c_{23} \\ c_{31} & c_{32} & {}_{33} \end{bmatrix} \tag{88}$$

$$\begin{aligned} c_{11} &= s\alpha c\alpha\dot{\alpha}(I_{xx_2} - I_{yy_2} - m_2 b^2) \\ c_{22} &= s\alpha c\alpha\dot{\theta}(I_{xx_2} - I_{yy_2} - m_2 b^2) \\ c_{21} &= -s\alpha c\alpha\dot{\theta}(I_{xx_2} - I_{yy_2} - m_2 b^2) \\ c_{13} &= c_{22} = c_{23} = c_{31} = c_{32} = c_{33} = 0 \end{aligned} \tag{89}$$

$$G = \begin{bmatrix} 0 \\ 9.81 m_2 a_2 c\alpha \\ 0 \end{bmatrix} \tag{90}$$

For Y_1,

$$Y_1 = M_2(q)\dot{\dot{q_r}} + C_2(q,\dot{q})\dot{q_r} + G_2(q) \tag{91}$$

$$M_2 = \begin{bmatrix} m_{11} & m_{12} & m_{13} \\ m_{21} & m_{22} & m_{23} \\ m_{31} & m_{32} & m_{33} \end{bmatrix} \tag{92}$$

$$\begin{aligned} m_{11} &= (a_2 c\alpha - g c\alpha\beta)^2 \\ m_{12} &= 0 \\ m_{13} &= 0 \\ m_{21} &= 0 \\ m_{22} &= a_2^2 + g^2 + 2a_2 g c\beta \\ m_{23} &= a_2 g c\beta + g^2 \\ m_{31} &= 0 \\ m_{32} &= a_2 g c\beta + g^2 \\ m33 &= g^2 \end{aligned} \tag{93}$$

$$C_2 = \begin{bmatrix} c_{11} & c_{12} & c_{13} \\ c_{21} & c_{22} & c_{23} \\ c_{31} & c_{32} & 33 \end{bmatrix} \tag{94}$$

$$\begin{aligned}
c_{11} &= -a_2^2 s\alpha c\alpha\dot{\alpha} - c\alpha\beta s\alpha\beta(\dot{\alpha}+\dot{\beta}) + a_2 g s\alpha\beta c\alpha(\dot{\alpha}+\dot{\beta}) + a_2 g s\alpha c\alpha\beta\dot{\alpha} \\
c_{22} &= -a_2^2 s\alpha c\alpha\dot{\theta} - g^2 s\alpha\beta c\alpha\beta\dot{\theta} + (a_2 g s\alpha c\alpha\beta + a_2 g c\alpha s\alpha\beta)\dot{\theta} \\
c_{13} &= -g^2 s\alpha\beta c\alpha\beta\dot{\theta} + \dot{\theta} a_2 g s\alpha\beta c\alpha \\
c_{21} &= -c_{12} \\
c_{22} &= a_2 g s\beta\dot{\beta} \\
c_{23} &= -a_2 g s\beta\dot{\alpha} - a_2 g s\beta\dot{\beta} \\
c_{31} &= -c_{13} \\
c_{32} &= a_2 g s\beta\dot{\alpha} \\
c_{33} &= 0
\end{aligned} \tag{95}$$

$$G = \begin{bmatrix} 0 \\ 9.81 a_2 c\alpha + 9.81 a_3 c\alpha\beta \\ 9.81 a_3 c\alpha\beta \end{bmatrix} \tag{96}$$

Similarly Y_2 , Y_3, Y_4 are also defined.

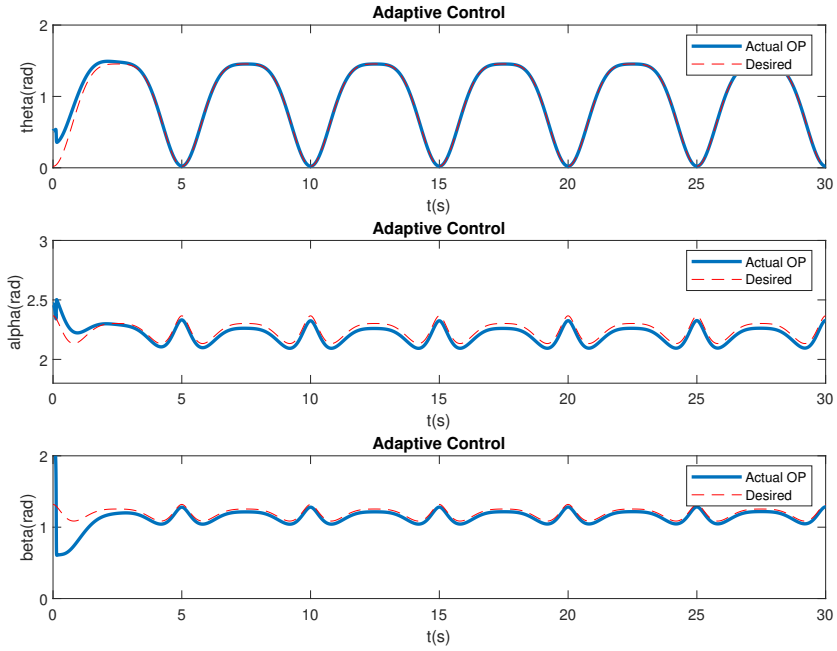

Figure 14: Position Plot- Adaptive Control

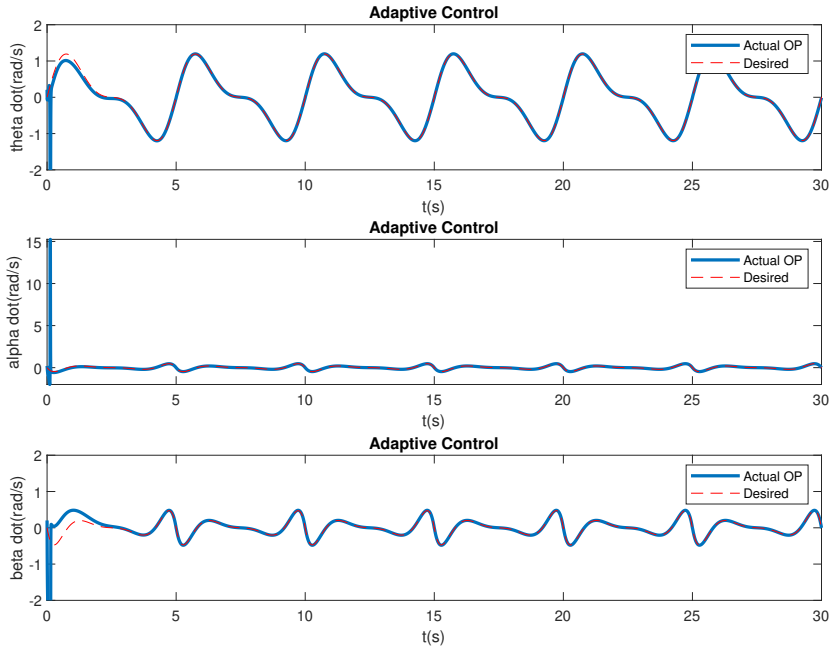

Figure 15: Velocity Plot- Adaptive Control

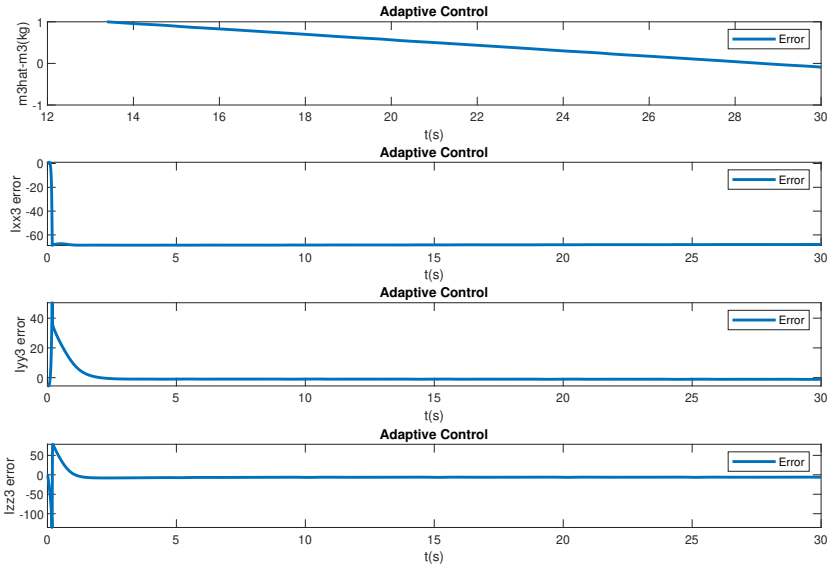

Figure 16: Convergence plots-Adaptive Control

Observation: Fig(14) and Fig(16) shows the actual trajectory traced by the robot arms in comparison with the desired trajectories. The adaptive controller is able to achieve convergence of the trajectories and velocities within 5 seconds, with controller gains of γ_1= 50, γ_2 =30, γ_3 = 20, γ_4 = 50 and K_d =20 respectively. The best estimates of m_3, I_{yy3}, I_{zz3} converge with their original values in 30,5 and 3 seconds respectively. However the best estimate of I_{xx3} does not converge with its original value.

8.4 Discussion

1. From the plots for regulation Fig(6) and Fig(7), it is seen that the PD controller action is able to hold the position of the robot arm at the desired joint angles. $K_p = 40$ and K_d =30 are the gains associated with holding the respective positions necessary. The convergence of the plots is achieved in about 5 seconds. The first couple runs of the robot can be used for tuning the robot and the robot should have good repeatability after that.

2. From the position and velocity plots of a computed and modified torque controller, it is observed that both the controllers are able to achieve convergence of parameters to the desired values. However, the modified computed torque controller has a quicker convergence time and also has lesser gains compared to the computed torque controller. Therefore, the modified computed torque controller is better for the considered application.

3. The robust controller has been demonstrated to show the controller response when the parameters of the robot have been overestimated by about 25%. This controller is able to achieve convergence but it has to be to taken into account that the initial errors are the highest for this controller. This points to using an adaptive controller with real time parameter adaptation.

4. The adaptive controller can be used when real time estimation of the parameters is needed. The adaptive controller is able to achieve the convergence in the unknown mass m_3 and the moments of inertia I_{yy3} and I_{zz3}. Convergence is not obtained with the moment of inertia, I_{xx3}. However, the adaptive controller is able to track the desired trajectory. The adaptive controller produces very little errors with respect to the trajectory generated. Convergence to the desired trajectory is achieved in about 3 seconds.

9 Conclusion and Future work

The report summarises the dynamics and motion of a 3DOF robotic arm. The forward and inverse kinematics have been setup for the robot arm. The potential and kinetic energies of the individual links of the robot have been calculated, which was used to set up the Lagrangian and equations of motion. Control techniques have been demonstrated to track the required trajectory and hold a required position. The trajectory modelled is a simple sweep. The trajectory modelled has only one drop location and then the robot returns back to the start location. Other trajectories can also be modelled similarly using a polynomial of the required degree. The trajectory can also be modelled with sin and cos functions. Obstacle avoidance has been demonstrated by a simple height manipulation. Obstacle avoidance can be done in a 3D space if the assumptions are tightened up. The same application can also be modelled with a 6DOF robot with a spherical wrist. This will offer a greater flexibility in operation. Controller tuning has not been implemented which would be good starting point for further work.

10 References

1. War War Naing, Kyi Zar Aung, Aung Thike, 'Position Control of 3 DOF Articulated Robot Arm using PID Controller', International Journal of Science and Engineering Applications(2018)

2. Pratik Baid, Manoj Kumar, 'A 3-DOF Robot arm for Drawing Applications', International Journal of Engineering Research and Technology(2016)

3. Sergei Evgenievich Ivanov, Tatiana Zudilova, Tatiana Voitiuk, Lubov Niolaevna Ivanova, 'Mathematical Modelling of the Dynamics of 3DOF Robot Manipulator with Software Control(2020)